JBC Papers in Press. Published on March 6, 2020 as Manuscript RA119.012063
The latest version is at https://www.jbc.org/cgi/doi/10.1074/jbc.RA119.012063

Substrate recognition and ATPase activity of the *E. coli* cysteine/cystine ABC transporter YecSC-FliY

Siwar Sabrialabed[1], Janet G. Yang[2], Elon Yariv[3], Nir Ben-Tal[3], and Oded Lewinson[1].

[1] Department of Biochemistry and the Rappaport Institute for Medical Sciences, Faculty of Medicine, The Technion-Israel Institute of Technology, Haifa, Israel
[2] Department of Chemistry, University of San Francisco, San Francisco, CA
[3] Department of Biochemistry and Molecular Biology, George S. Wise Faculty of Life Sciences, Tel Aviv University, Tel Aviv, Israel

For correspondence: lewinson@technion.ac.il

Running title: The *E. coli* cysteine/cystine ABC transporter YecSC-FliY

Keywords: membrane protein, enzyme mechanism, ABC transporter, ATPase, amino acid transport, sulfur, membrane transport, enantiomers, YecSC-FliY, cysteine/cystine import.

Abstract

Sulfur is essential for biological processes such as amino acid biogenesis, iron–sulfur cluster formation, and redox homeostasis. To acquire sulfur-containing compounds from the environment, bacteria have evolved high-affinity uptake systems, predominant among which is the ABC transporter family. Theses membrane-embedded enzymes use the energy of ATP hydrolysis for transmembrane transport of a wide range of biomolecules against concentration gradients. Three distinct bacterial ABC import systems of sulfur-containing compounds have been identified, but the molecular details of their transport mechanism remain poorly characterized. Here, we provide results from a biochemical analysis of the purified Escherichia coli YecSC-FliY cysteine/cystine import system. We found that the substrate-binding protein (SBP) FliY binds L-cystine, L-cysteine, and D-cysteine with micromolar affinities. However, binding of the L- and D-enantiomers induced different conformational changes of FliY, where the L- enantiomer/SBP complex interacted more efficiently with the YecSC transporter. YecSC had low basal ATPase activity that was moderately stimulated by apo-FliY, more strongly by D-cysteine–bound FliY, and maximally by L-cysteine– or L-cystine–bound FliY. However, at high FliY concentrations, YecSC reached maximal ATPase rates independently of the presence or nature of the substrate. These results suggest that FliY exists in a conformational equilibrium between an open, unliganded form that does not bind to the YecSC transporter, and closed, unliganded and closed, liganded forms that bind this transporter with variable affinities yet equally stimulate its ATPase activity. These findings differ from previous observations for similar ABC transporters, highlighting the extent of mechanistic diversity in this large protein family.

Introduction

ABC transporters comprise one of the largest protein families of any proteome, and play diverse and vital roles in all kingdoms of life (1–3). These membrane-embedded enzymes use the energy of ATP hydrolysis to transport a wide range of biomolecules against their concentration gradients (4–6). In humans, genetic defects in ABC transporters lead to diseases such as Tangier disease, adrenoleukodystrophy and cystic fibrosis (7–9) and their elevated expression underlies the phenomenon of tumor multidrug resistance (10, 11).

It is therefore of no surprise that decades of research were dedicated to understanding their structure and function. Despite the diversity of their physiological roles and substrate recognition profiles (12–17) ABC transporters share a common basic architecture, minimally comprising of two intracellular nucleotide-binding domains (NBDs) that bind and hydrolyze ATP, and two transmembrane domains (TMDs) that form a substrate-translocation pathway (18–21). ATP is bound at two composite sites formed at the interface of the NBDs, and proper formation of the ATP-binding sites requires that the NBDs close into a tight head-to-tail sandwich (22). Binding and hydrolysis of ATP drives the transition of the TMDs between inward- and outward-facing conformations with concomitant changes of substrate-binding affinities (23–25). Thus, for an exporter the inward-facing conformation will have the higher substrate-binding affinity which will be lowered upon transition to the outward-facing conformation, and *vice-versa* in an importer. Binding of the substrate generally promotes the closure of the NBDs and subsequent ATP hydrolysis (26–28), and this allosteric communication provides a positive feedback mechanism for substrate translocation.

ABC transporters that function as importers are found almost exclusively in prokaryotes (6, 29). The importers do not bind their substrates directly, but rather work in concert with a substrate-binding protein (SBP). The SBP binds the substrate with high affinity, delivers it to the transporter and largely dictates the transport specificity (20, 29, 30). Although there are exceptions (31, 32), each SBP is specific for one transporter and together they form the functional transport unit. In bacteria, ABC importers are major determinants for high affinity acquisition of essential nutrients (33–36). Their function becomes essential in nutrient-depleted environments and therefore many

bacterial ABC import systems are directly linked to bacterial virulence and pathogenesis (37–39).

Sulfur is an essential element for all life forms, and bacteria are no exception. It is used for synthesis of amino acids, in iron-sulfur clusters, as a redox reactant, and in coordination of transition metals such as zinc and copper (40, 41). Because of the unique chemical properties of sulfur it cannot be readily substituted by other elements, and therefor to satisfy their sulfur quota bacteria evolved elaborate mechanisms for sensing, acquiring, and assimilating sulfur atoms (42–45). Sulfur-containing organic compounds such as cysteine and its oxidized dimeric form cystine, glutathione (GSH), and aliphatic sulfonates provide important sulfur sources for bacteria (42, 46). Under conditions of sulfur limitation, CysB, which is a LysR-type transcriptional regulator upregulates the expression of various uptake systems that are specific for importing sulfur-containing organic compounds (47). Among these are the ABC transport systems *tauABC*, *ssuABC*, and yecSC-*fliY* that import taurine, aliphatic sulfonates and cysteine/cystine, respectively (48–50). The importance of the three systems in acquiring sulfur under cysteine/sulfur starved conditions and in redox homeostasis have been demonstrated by determining the growth phenotype of deletion strains and by uptake of radio-tracer by whole cells (49). However, their molecular-level biochemical understanding remains limited, likely because of the technical challenges often associated with working with membrane proteins.

Here, we describe the overexpression and purification of the components of the *yecSC-fliY* ABC cysteine/cystine importer (50). Using the purified components we investigated the substrate recognition profile of FliY (the SBP), with an emphasis on discrimination between the L- and D-enantiomers of cysteine and cystine. We characterized the ATPase activity of the transporter, and its modulation by the SBP and the L- and D-enantiomers. We describe a mechanism of tight coupling between ATP hydrolysis and the presence of the SBP, and selective stimulation of ATP hydrolysis by the L-enantiomers.

Results

Recognition profile of FliY, the substrate binding protein (SBP) of the system

In ABC importers, transport specificity is almost exclusively determined by the binding specificity of the substrate binding protein (SBP). The SBP binds the substrate with high affinity and delivers it to the membrane-embedded transporter (4, 5). In Gram-positive bacteria the SBP is either tethered to the membrane via a lipid anchor or fused directly to the transporter. In Gram-negative bacteria, the SBP is a soluble periplasmic protein (15, 51, 52). To study the recognition spectrum of the YecSC-FliY import system, we first over-expressed and isolated the FliY SBP. Following induction with IPTG whole cells lysates showed a dramatic enrichment of two protein bands (SI Figure 1A). The higher band is presumably the immature form of the SBP, which includes an intact N-terminal signaling sequence. The lower band is most likely the mature SBP, in which the signal sequence is cleaved upon secretion to the periplasm. The presence of both species in whole cell lysates suggests that the high levels of overexpression lead to an overflow of the protein export machinery and accumulation of cytosolic immature FliY. Indeed, the higher molecular band was absent from the periplasmic extract and the mature protein was subsequently purified to homogeneity by Ni-NTA chromatography (SI Figure 1B). The purified protein was highly mono-disperse in size exclusion chromatography indicting a single molecular species that approximately corresponds in size to the monomeric form of FliY (SI Figure 1C).

We then used two independent methods to measure substrate binding by FliY: nano differential scanning fluorimetry (nanoDSF) and isothermal titration calorimetry (ITC). nanoDSF is based on the observation that the thermal stability of a protein is increased upon ligand binding (53, 54). By exciting the protein at 280 nm and measuring the ratio of 350 nm and 330 nm fluorescence intensities while heating at a constant rate, one can determine the protein denaturation midpoint (Tm). This experiment is conducted in the absence and presence of a potential ligand, and a binding event is detected by a shift of the Tm to a higher temperature. When two different ligands induce substantially distinct bound conformations, the magnitude of the shift of the Tm will differ. Thus nanoDSF can

resolve different ligand-bound conformations under saturating conditions. In contrast to nanoDSF, ITC directly measures ligand binding by the measuring the amount of heat released or absorbed during a binding event. ITC is considered a benchmark method in measuring of protein-ligand interactions (55, 56). The combination of these two approaches (nanoDSF and ITC) provides complimentary information on a protein-ligand interaction event.

Previous *in vivo* growth studies suggested that the FliY-YecSC ABC transport system satisfies the sulfur requirements of *E. coli* by importing a variety of compounds such as the amino acid cysteine, its oxidized dimeric form cystine, djenkolic acid, and lanthionine (49, 50). We therefore studied the binding of various sulfur-containing compounds by FliY.

In the absence of ligand, FliY was a relatively stable protein, with a Tm of ~65 C°. The nanoDSF measurements were highly reproducible as indicated by the near-perfect superimposition of replicates (SI Figure 2). As expected, addition of non-related substrates such as D-maltose or D-arabinose had no thermo-stabilizing effect (SI Figure 2). In contrast, addition of L-cysteine led to a significant stabilization of the SBP by ~4.5 C° (Figure 1A). Next, we tested the amino acid serine, which is identical to cysteine except for the absence of the sulfur atom from its side chain. Despite this similarity, L-serine had no thermo-stabilizing effect on FliY, suggesting that the sulfur atom is an important determinant of FliY recognition (Figure 1A). However, other sulfur-containing compounds such as, L-methionine, glutathione, or djenkolic acid had no thermo-stabilizing effect, demonstrating the specificity of the FliY-L-cysteine interaction (Figure 1A). Similar to L-cysteine, addition of the L-enantiomer of its oxidized dimeric form (Cys-S-S-Cys, cystine) also led to thermo-stabilization of FliY (Figure 1B). However, for both cysteine and cystine the effect was highly stereo-specific, as no thermo-stabilization effect was observed in the presence of either D-cysteine or D-cystine (Figure 1B). Taken together, the nanoDSF results suggest that FliY specifically binds the L-enantiomers of the amino acid cysteine and its oxidized dimeric form (L-cystine).

Next, we used ITC to measure the binding affinity of FliY to different ligands. Titration of L-cystine to apo-FliY generated a strong exothermic signal (Figure 2A), and a fit with a simple 1:1 interaction model yielded a K_D value of 9.3±2.8 μM. This binding affinity is similar to published values for other amino acid SBPs, such as the L-glutamine SBP of *L. monocytogenes* (K_D = 4.7 μM), yet considerably weaker than that reported for the *E. coli* SBPs for L-histidine (HisJ, K_D = 60 nM) and for L-methionine (MetQ, K_D = 0.2 nM) (57–59). This variability in binding affinities between SBPs of amino acids may reflect the environmental availabilities of the amino acids. The binding of L-cystine by FliY was entirely enthalpy-driven, and a positive entropic value was noted in all the experiments. Although we did not attempt to pinpoint the values of ΔH and ΔS, these observations are in line with the suggestion that the mobility of class-II substrate binding proteins such as FliY is restricted upon ligand binding (therefore leading to a decrease in ΔS). Consistent with nanoDSF results, titration of D-cystine to apo-FliY did not produce any measurable ITC signal (Figure 2B). From these results we conclude that FliY binds L-cystine, but not its D-enantiomer.

Next, we conducted similar experiments with the L- and D- enantiomers of cysteine. As expected, the binding of L-cysteine by FliY was readily detectable by ITC (Figure 2C), was also exothermic, and mainly driven by enthalpy. The affinity of FliY to L-cysteine (K_D=14.4 ± 2.4 μM) was modestly weaker (1.5-fold) than for L-cystine, yet this difference was determined to be significant using a student's two-sided T-test (p = 0.02). Surprisingly, the binding of D-cysteine to apo-FLiY was readily detected by ITC experiments (Figure 2D). The affinity of FliY to D-cysteine (K_D = 10 ± 3.4 μM) was similar to the affinities measured for L-cystine and L-cysteine.

With respect to binding affinity of D-cysteine, the contradiction between the ITC and nanoDSF results was puzzling. We hypothesized that D-cysteine binds at the same site as L-cysteine or L-cystine, but that binding of D-cysteine induces a distinct conformational change that does not lead to increased thermostability. Recent studies have indeed demonstrated that binding of closely related substrates by SBPs can lead to different bound conformations (17, 60, 61). To explore this possibility, we conducted binding competition experiments using

nanoDSF. In these experiments, a four-fold molar excess of D-cysteine was added together with L-cysteine. We predicted that if D-cysteine binds to the same site as L-cysteine but does not stabilize FliY, its presence will inhibit the stabilization effect mediated by binding of L-cysteine. Consistent with this prediction, relative to the presence of only L-cysteine, the concomitant addition of both enantiomers led to a reproducible ~2 C° reduction in thermostability (Figure 3A).

As a negative control, we repeated this experiment using L-methionine as a competitive ligand and did not observe a reduction in thermostability. Furthermore, competition experiments using D-cystine had no effect on the thermo-stabilization of FliY by L-cystine (Figure 3B).

Perhaps unexpectedly, the mixture of D-cysteine and L-cysteine did not lead to formation of multiple or broader peaks, but rather to formation of a single peak of comparable width, yet of reduced thermostability. Given the capacity of FliY to bind cystine, a putative explanation for this phenomenon may be the concurrent binding of D-cysteine and L-cysteine which leads to an intermediate level of stabilization.

Taken together, the ITC, nanoDSF, and nanoDSF-competition results suggest that FliY specifically binds L-cystine, L-cysteine, and D-cysteine, and that the binding of the L-enantiomers leads to a conformational change that is distinct from that induced by binding of the D-enantiomer.

ATP hydrolysis by YecSC

ABC transporters that function as importers are divided into two classes, or "types." Type-I importer systems import sugars, amino acids, and peptides (36, 62–65), while Type-II systems import metals or organo-metal complexes such as heme, siderophores, and vitamin B_{12} (15, 66–68). The Type-I and Type-II sub-groups differ structurally and mechanistically, and one distinctive mechanistic feature is their ATP hydrolysis activity. Type-I ABC importers generally have low basal rates of ATP hydrolysis that are greatly stimulated by docking of the substrate-loaded SBP (69–71). In contrast, the Type-II importers have very high basal rates of ATP hydrolysis that are much less responsive to the SBP and/or substrate (23, 34, 35, 72). To characterize the basal ATP hydrolytic activity of YecSC and its modulation by FliY, the transporter was overexpressed in *E. coli*. Following the strategy originally developed by Locher and co-workers (73) we screened multiple constructs of YecSC to identify the positions that can accommodate the His-tag without interfering with the membrane-embedded expression of the transporter. In this screen we observed that tagging of the NBD at its C-terminal completely abolished its expression, and that the TMD domain tolerates tagging at both termini (SI Figure 3). When we compared the expression of the singly-tagged constructs, the N-terminally tagged NBD showed greater expression than tagged TMD constructs (SI Figure 3). Therefore, for subsequent studies we focused on the construct where only YecC (NBD) is His-tagged while YecS (TMD) is tag-free.

To extract YecSC from *E. coli* membranes, several detergents were screened. Of these, the most efficient extraction was achieved using CYMAL-7 (7-Cyclohexyl-1-Heptyl-β-D-Maltoside), and YecSC could be subsequently purified to high homogeneity in this detergent. However, despite the clear presence of both the ATPase and transmembrane domains we could not detect any ATPase activity of CYMAL-7 - purified YecSC. Other detergents did not efficiently extract YecSC from membranes, and we therefore tested combinations of detergents. We found that a 1:1 (w/w) mixture of DM (N-Decyl- β -D-Maltopyranoside) and DDM (N-Dodecyl- β -D-Maltopyranoside) improved the extraction of YecSC and allowed for isolation of the transporter with high purity (SI Figure 4). To preserve the ATPase activity of YecSC, it was necessary to add lipids to the DDM/DM-purified protein. All subsequent activity measurements were conducted in the presence of a 20:1 molar excess of purified *E. coli* polar lipids.

In the absence of FliY, YecSC displayed very low ATP hydrolytic activity that was barely detectable above the background level (Figure 4A). Addition of L-cystine alone (in the absence of FliY) had no effect, and the ATPase activity remained near background. In contrast, addition of a 5-fold molar excess of substrate-free apo-FliY led to a marked (~3-fold) stimulation of the ATPase activity of YecSC. To rule out the possibility of contaminating ATP hydrolysis activity, we conducted experiments where FliY was present but YecSC was absent. No ATPase

activity was measured in these experiments, demonstrating that the observed activity requires the presence of both YecSC and FliY. Concomitant addition of both FliY and L-cystine led to the highest level of stimulation, approximately 11-fold over basal activity (Figure 4A).

Next, to examine the role of the two ATPase sites in YecSC, we measured the initial rates of activity under a range of ATP concentrations. As shown, at ATP concentrations of 15-2000 μM, the initial rates of ATP hydrolysis were linear for more than 2 minutes (Figure 4B). The rate constants were plotted as a function of ATP concentration, and the data were fit using either the Michaelis–Menten model or an expanded version that includes the Hill coefficient (Figure 4C). Adding the term for the Hill coefficient lowered the RMSD of the fit by ~15-fold. These results suggest that the two ATP binding sites of YecSC are interdependent and hydrolyze ATP cooperatively (n_{HILL}=1.7 ± 0.2). Similar cooperative ATP hydrolysis has been described for the vitamin B_{12} transporter BtuCD (n_{HILL}= 2), the methionine transporter MetNI (n_{HILL}=1.7), the maltose importer $MalFGK_2$ (n_{HILL}= 1.4 - 1.7), and the histidine importer HisPQM (n_{HILL}= 1.9) (16, 69, 72, 74). The affinity of YecSC to ATP is quite low ($Km_{(ATP)}$ ≈ 0.3 mM), substantially weaker than that reported for BtuCD and $MalFGK_2$ (10-20 μM), yet similar to the *Km* reported for HisPQM (≈ 0.5 mM) and MetNI (≈ 0.3 mM) (16, 35, 69, 70, 72). Given the high intracellular concentrations of ATP in *E. coli*, we anticipate that YecSC would be nearly saturated with ATP under physiological conditions (75).

As shown above (Figure 4A), substrate-bound FliY more strongly stimulates the ATPase activity of YecSC than substrate-free FliY. Previous work has demonstrated that class-II substrate binding proteins undergo a large Venus flytrap-like conformational change when binding substrates (76–79). This conformational change is sensed by the transmembrane domain of the transporter and provides a substrate-occupancy signal that is transmitted to the nucleotide binding domains. As a result, docking of the substrate-bound SBP stimulates ATP hydrolysis and ultimately transport (70). This substrate-dependent stimulation of ATPase activity can be a result of two mechanisms or their combinations. One possibility is that substrate-free and -bound FliY dock to YecSC with similar affinities, yet substrate-bound FliY more efficiently induces the closure of the NBDs and thus promotes ATP hydrolysis. Such a mechanism has been demonstrated for the ABC importers for maltose and histidine (25, 80). Alternatively, substrate binding could increase the affinity of FliY to YecSC, which leads to a higher fraction of transporter-bound FliY molecules in the ATPase assays.

To discriminate between these two possibilities, we determined the initial rates of ATP hydrolysis with a range of FliY concentrations in the absence or presence of saturating L-cystine. Under both conditions the data was readily fit with the Michaelis–Menten equation, consistent with a 1:1 FliY-YecSC interaction ratio (Figure 5A). A comparison of the kinetic constants showed that the apparent k_{cat} was largely unaffected by the presence of substrate. In contrast, the presence of substrate lowered the apparent K_M for FliY by ~9-fold (from 10.3 to 1.1 μM). The unchanged k_{cat}^{app} and the lower K_M^{app} suggest that once docked, apo- and holo-FliY equally stimulate the ATP hydrolysis activity of the transporter, but that L-cysteine bound-FliY has higher affinity to YecSC than apo-FliY.

In nanoDSF and ITC binding experiments with FliY, we observed that the L- and D- enantiomers of cystine and cysteine bind differently, which could lead to distinct conformations of holo-FliY. In turn, this difference in conformations could influence the stimulation of ATP hydrolysis by YecSC. To test this hypothesis, we measured the stimulation of ATPase activity by each of these substrates. As anticipated based on our thermodynamic measurements, D-cystine had no effect on the FliY-mediated stimulation of ATPase activity (Figure 5B). This observation further supports the conclusion that FliY does not interact with D-cystine. The highest levels of ATPase stimulation were observed in the presence of the L-enantiomers of cysteine and cystine (Figure 5B), suggesting a productive interaction of FliY with the L-enantiomers. Finally, FliY-D-cysteine had a modest (yet reproducible) stimulatory effect, which was higher than the effect of FliY alone yet lower than the effect of the L-enantiomers, further supporting the hypothesis that binding of

D-cysteine leads to a distinct conformational change.

3-D structural modelling of FliY

As described above, FliY binds both enantiomers of cysteine (but not the iso-structural serine), yet discriminates between the L- and D-enantiomers of cystine, binding only the former. In an attempt to understand the molecular basis of this selectivity we employed a combination of 3-D structural modelling, evolutionary analysis, and molecular docking. Notably, since cystine is twice larger than cysteine FliY may adopt different conformations when binding each of these two ligands. We therefore used two different templates for the modeling, as described below.

Multiple sequence alignment of the query protein and its homologues facilitates homology modeling both in that it may aid in finding the best structural template and in improving the query-template alignment. Thus, we used HHblits (81) to search for homologues of FliY, and a search against Uniclust30 (82) yielded 250 homologs, which we aligned using MAFFT (83). We then used Modeller (84) to construct a model of FliY using the 2.26Å resolution crystal structure of NGO2014, the L-cysteine SBP of *Neisseria Gonorrhoeae* (PDB ID: 2YJP, 26% sequence identity to FliY, (85).

We then docked L-cysteine to this model (see methods for docking protocol) and observed that according to the model, the C-terminus of L-cysteine makes a salt bridge with the side chain of R114, its N-terminus makes hydrogen bonds with T109 and D192, and the thiol forms hydrogen bonds with Y51 and T158, and a weak salt bridge, 4.3Å in length, with K182 (Figure 6A). Docking of D-cysteine revealed that it docks in essentially the same pose as L-cysteine (Figure 6B), which explains why FliY binds both enantiomers. The predicted pKa (see methods) for the docked cysteine was estimated to be 6, suggesting that 95 percent of the bound cysteine population would be deprotonated at physiological pH. This may also explain why serine, with its much higher pKa of 15, is discriminated against: at physiological pH, serine's side chain will be protonated and will thus make less favorable interactions with the side chains of Y51, T158 and K182.

We used a similar protocol and the structure of the L-cystine SBP from *Neisseria Gonorrhoeae* (PDB ID: 2YLN, 35% sequence identity to FliY, (85) to predict the coordination of L-cystine by FliY. The predicted binding mode for L-cystine was very similar to what was observed in the template structure (Figure 6C), while the pose predicted for D-cystine differed in its interaction with E48 (Fig 6D). The electrostatic interaction between the amine of L-cystine and the carboxylate oxygens of E48 seems pivotal as it is conserved in all FliY homologues (ConSurf grade of 9 on a scale of 1-9,(86) and also in the L-cystine SBP of *Neisseria Gonorrhoeae* (here the equivalent residue is E56*).* Whereas the amine of L-cystine interacts with both carboxylate oxygens (Figure 6C), in D-cystine the amine is displaced and can only interact with one oxygen atom (Fig 6D). This difference in binding modes may explain why FliY preferentially binds the L enantiomer of cystine.

Discussion

Previous studies suggested that SBPs of ABC transporters may exist in a conformational equilibrium between an open-unliganded form (O), a closed-unliganded form (C), and a closed-liganded form (C · L) (17, 61, 87). The results we present here for YecSC-FliY are consistent with such a model (Figure 7).

In the absence of ligand, FliY predominantly adopts the O conformation, which does not bind to YecSC. The small fraction of molecules that are in the C conformation are available for docking to YecSC and stimulate its ATPase activity. In the presence of ligand, the conformational equilibrium is shifted toward the (C · L) conformation. More molecules are now available for docking to YecSC and higher ATPase stimulation is observed. This is why the affinity of FliY to YecSC appears to be higher in the presence of ligand. However, it is important to note that in terms of ATPase-stimulation the C and C · L conformations are equivalent. At high enough concentrations APO-FliY stimulates the ATPase activity of YecSC just as well as HOLO-FliY (Figure 5A). The only effect of substrate is to shift the equilibrium between the O and C states. This is different from what had been suggested for the maltose transporter, where both the SBP and maltose are required to induce the

closure of the NBDs (70). In MalFGK, the ligand (maltose) has a direct role in the allosteric communication via its interaction with residues in the trans-membrane domain (88, 89). This substrate-mediated direct effect seems to be missing in YecSC-FliY since full stimulation of ATP hydrolysis can also be achieved in the absence of ligand. Binding of D-cysteine seems to lead to a distinct ligand bound form; C* · L, with different thermostability and a reduced ATPase stimulatory effect. A recent single-molecule study suggested that binding of cognate and non-cognate substrates by SBPs lead to productive and non-productive conformational changes, respectively (61). This may indicate that although D-cysteine is bound by FliY it is not transported by YecSC, or transported with reduced efficiency. This issue remains to be resolved by transport assays.

On the one hand, the results we report here for the cysteine/cystine importer YecSC-FliY are very similar to those reported for the histidine ABC importer HisPQM-J (69): both systems hydrolyze ATP cooperatively with very similar Hill coefficients and nearly identical affinity to ATP. However, the effect of ligand is reversed in the two systems. In HisPQM, apo and holo HisJ bind to the transporter with equal affinities, but the Vmax of ATP hydrolysis is ~13-fold higher in the presence of histidine (69). The opposite is true for YecSC-FliY where substrate increases the affinity of the SBP to the transporter by ~9-fold but has no effect on the Vmax of ATP hydrolysis. These differences provide further demonstration of the extent of mechanistic diversity in the super-family of ABC transporters (4).

An additional difference between YecSC-FliY and other ABC transporters of amino acids is related to the complete absence of cysteine from the amino acid sequence of YecSC-FliY and other cysteine import systems. The same cannot be said for glutamine, histidine, or methionine which are routinely found in the amino acid sequence of the ABC importers that import them. This means that even when the intracellular level of cysteine is low, upregulated biogenesis YecSC-FliY can be fulfilled, leading to replenishing of the cysteine pool.

Furthermore, the YecSC-FliY system is distinct in the selectivity of the SBP. Relative to FliY, other SBPs of amino acids display much higher discrimination in favor of the L-enantiomer. For example, GlnP of *L. monocytogenes* and HisJ of *E. coli* bind only the L-enantiomers of glutamine or histidine, respectively (57, 90). Similarly, the affinity of MetQ to L-methionine is ~15000-fold higher than to the D-methionine (91). In comparison, the affinity of FliY to L-cysteine is only ~3-fold higher than to D-cysteine. Why would FliY be more permissive towards the D-enantiomer? FliY expression is induced under conditions of limited sulfur availability (92) and *E. coli* contain several enzymes dedicated to the utilization of D-cysteine as a sulfur source, including D-cysteine desulfhydrase (93). This observation suggests that a main goal of cysteine import systems is to deliver the sulfur atom in addition to a proteogenic precursor. In this respect, D-cysteine contains the precious sulfur atom just the same, and to ensure sufficient supply of sulfur bacteria may have evolved to import also the non-proteogenic D-enantiomer.

Experimental procedures

Bacterial Strains and Plasmids

The genes for *yecC* (ACC P37774), *yecS* (ACC P0AFT2), and *fliY* (ACC P0AEM9) were PCR-amplified from the *E. coli* K-12 derivative strain BW25113. All restriction sites for subcloning were inserted at this stage. *fliY* was inserted into the *NdeI/XhoI* sites of a pET21b expression vector, resulting in a C-terminal fusion of a 6x-histidine tag. *yecS* and *yecC* were inserted in tandem into a custom-made pET-derived vector where each gene is preceded by a T7 promoter and a ribosome binding site (RBS). The YecSC construct used in this study contained an enterokinase cleavage site followed by 10x-histidine tag fused to the N-terminal of YecC.
E. coli strain DH5α (Invitrogen) was used for cloning procedures and BL21-Gold (DE3) (Stratagene) was the host for protein expression.

Protein expression and purification

For small-scale expression testing, 20 mL cultures were grown in glycerol-supplemented Terrific Broth media to an OD_{600} of ~2 and induced for 1.5 h with 0.5 mM IPTG. Membranes were prepared by disrupting the cells by sonication, debris removal by centrifugation for

10 min at 10,000 xg, and membrane sedimentation by ultracentrifugation at 120,000 × g for 45 min. The His-tagged protein content of the membrane fractions was visualized using standard SDS-PAGE and immunoblot detection using an anti-His antibody. To visualize the expression of FliY cells were disrupted as above, debris removed, and 30-50 μg of the total cell lysate was separated by SDS-PAGE and stained with Coomassie brilliant blue.

Purification of FliY. Osmotic shock extracts prepared from cells overexpressing FliY in 50 mM Tris-HCl pH 7.5, 250 mM NaCl, 20 mM imidazole pH 8 were loaded over-night onto a 5 mL Ni-NTA affinity column (HisTrap HP, GE Healthcare). The column was washed with 20 CV of 20 mM imidazole before elution with a gradient of 60-250 mM imidazole. Imidazole was removed using a Sephadex G-25 column and FliY was concentrated using Amicon Ultra concentrator (Millipore) with a molecular cutoff of 30 kDa to 5-6 mg/mL. Aliquots of FliY were snap-frozen in liquid nitrogen and stored in –80 °C until use.

Purification of YecSC. For preparation of membrane fraction, cells were resuspended in 50 mM Tris·HCl pH 7.5, 0.5 M NaCl, 30 μg/mL DNase (Worthington), one complete EDTA-free protease inhibitor mixture tablet (Roche), 1 mM $CaCl_2$, 1 mM $MgCl_2$, and tip-sonicated for 30 min prior to rupture by three passages in an EmulsiFlex-C3 homogenizer (Avestin). Debris was removed by 30 min centrifugation (4 °C, 10,000 × g) and membranes were pelleted by ultracentrifugation at 160,000 × g for 1 h, washed and resuspended in 50 mM Tris·HCl pH 7.5, 0.5 M NaCl, and 10% (vol/vol) glycerol; and stored in –80 °C until use.

To solubilize the membranes, DM (N-Decyl-b-D-Maltopyranoside) and DDM (N-Dodecyl-b-D-Maltopyranoside) were each added to a final concentration of 0.5% (W/W). The suspension was gently tilted at 4 °C for 1 h and the insoluble fraction was removed by ultracentrifugation at 160,000 × g for 1 h. The soluble fraction was loaded onto a 5 mL Ni-NTA column as described above for FliY running Tris·HCl pH 7.5, 0.5 M NaCl, 0.05% DDM and 0.05% DM. The column was washed with 20 CV of the same buffer containing 20 mM imidazole, followed by 10 CV wash with buffer containing 60 mM imidazole. YecSC was eluted using an imidazole gradient of 60-250 mM, imidazole removed by desalting, protein concentrated to ~1 mg/mL using Amicon Ultra concentrator (Millipore) with a molecular cutoff of 100 kDa. Aliquots of YecSC were snap-frozen in liquid nitrogen and stored in –80 °C until use.

nanoDSF measurements

To remove potential co-purified endogenous ligands purified FliY was dialyzed over-night (2 buffer replacements) against 1000-fold excess of 50 mM Tris-HCl pH 7.5, 250 mM NaCl. The dialysis buffer was used to dilute the stock solutions of the tested ligands. FliY was incubated with different ligands and the Measurements were performed with Prometheus NT.48 (Nanotemper). The tryptophan residues of the protein were excited at 280 nm and the fluorescence intensity was recorded at 330 and 350 nm. The temperature of the measurement compartment increased from 25 to 95 °C at a rate of 1 °C min−1.

Isothermal titration calorimetry (ITC)

Prior to experiments, FliY was dialyzed over night against a 1000-fold (2 buffer replacements) volume of 50 mM Tris·HCl pH 7.5, 0.5 M NaCl. To avoid buffer mismatch, this dialysis buffer was used to dilute the stock solutions of the tested ligands. Calorimetric measurements were performed with MicroCal iTC200 System (GE Healthcare), and all measurements were carried out at 25 °C. 2 μL aliquots from a 200-400 μM (as indicated) ligand solution were added by a rotating syringe to the reaction well containing 200 μL of 70 μM FliY. Data fitting was performed with the Origin software using a simple 1 : 1 binding model, where the ligand-free form of the protein is in equilibrium with the bound species.

ATPase assays

ATP hydrolysis was performed using the EnzChek® Phosphate Assay Kit (Molecular probes). The reaction buffer contained 50 mM Tris·HCl pH 7.5, 0.5 M NaCl, 0.05% DDM, 0.05% DM, 20 μM *E. coli* polar lipids, 0.2 mM MESG (2-amino-6-mercapto-7-methylpurine riboside) 1 unit/mL PNP (purine nucleoside phosphorylase), and the indicates concentrations of ATP, YecSC, and FliY. Measurements were conducted at 37 ˚C in an automated plate reader

(Infinite M200 pro, Tecan). Following 2-5 min incubation at 37 ˚C 2 mM $MgCl_2$ was injected to initiate ATP hydrolysis.

Homology modelling

Multiple sequence alignment (MSA) of the query protein and its homologues facilitates homology modeling both in that it may aid in finding the best structural template and in improving the query-template alignment. Thus, we used HHblits (81) to search for homologues of the *Escherichia Coli* cysteine binding protein (FliY, SWISSPROT ID: P0AEM9). A search against Uniclust30 (82) yielded 250 homologs, which we aligned using MAFFT (83). Using the 2.26Å resolution crystal structure of NGO2014, the cysteine binding protein of *Neisseria Gonorrhoeae* (85) (PDB ID:2YJP, 26% sequence identity to FliY) and the 1.12Å resolution crystal structure of NGO0230, the cystine binding protein from the same bacteria (PDB ID: 2YLN, 35% sequence identity to FliY) as templates, we constructed homology models using modeler (84). The FliY, 2YJP and 2TLN multiple alignment and the coordinates of the homology models are provided as Suppl.

Molecular docking

Prior to any docking simulations, we had to prepare the homology models and template structures for docking using the protein preparation wizard (94). We mostly used the recommended settings for the preparation, except for the minimization, which was restricted to the hydrogen atoms – the heavy atoms were maintained in their crystal structure coordinates. The ligands were prepared using LigPrep (95) (Schrödinger LLC, NY, USA), which generated probable protonation states at pH 7.0±2.0. In this pH range, serine had a single protonation state (zwitterion with neutral sidechain) while the cysteine had two (protonated and deprotonated sidechain). Using Glide (96), we defined the receptor grid as a box with 10Å edges, centered around the ligand coordinates from the template structure. We then used the standard precision Glide docking protocol and generated up to five docking poses per ligand.

pKa calculations

To determine the pKa of the bound cysteine and serine ligands we used the DelPhiPKa webserver (97), which calculates the amino acids pKa within the context of the protein environment. We used the default settings to calculate the pKa of all the titratable residues, including serine, tyrosine, threonine and cysteine. Heteroatoms were removed, excluding the cysteine ligand, which was treated as part of the protein.

Conservation of coordinating residues

Amino acid conservation grades were calculated for the homology models and the template structures (PDB ID: 2YJP, 2YLN) using the ConSurf webserver (86), with default settings, except for the number of collected homologs which was increased to 300.

Data availability

All data presented are contained within the manuscript.

Funding and additional information

This work was supported by grants from the United States-Israel Binational Science Foundation (BSF) grant reference 2015102 (OL) and North Atlantic Treaty Organization (NATO) NATO (SPS Project G4622, OL, NBT).

Conflict of interest

The authors declare no conflict of interest.

References

1. Higgins, C. F. (1992) ABC transporters: from microorganisms to man. *Annu. Rev. Cell Biol.* **8**, 67–113
2. Dassa, E., and Bouige, E. (2001) The ABC of ABCs: a phylogenetic and functional classification of ABC systems in living organisms. *Res. Microbiol.* **152**, 211–229
3. Holland, I. B., Cole, S. P. C., Kuchler, K., and Higgins, C. F. (2003) ABC proteins: From Bacteria to Man
4. Lewinson, O., and Livnat-Levanon, N. (2017) Mechanism of Action of ABC Importers: Conservation, Divergence, and Physiological Adaptations. *J. Mol. Biol.* 10.1016/j.jmb.2017.01.010
5. Locher, K. P. (2016) Mechanistic diversity in ATP-binding cassette (ABC) transporters. *Nat. Struct. Mol. Biol.* **23**, 487–93
6. ter Beek, J., Guskov, A., and Slotboom, D. J. (2014) Structural diversity of ABC transporters. *J. Gen. Physiol.* **143**, 419–35
7. Rust, S., Rosier, M., Funke, H., Real, J., Amoura, Z., Piette, J.-C., Deleuze, J.-F., Brewer, H. B., Duverger, N., Denèfle, P., and Assmann, G. (1999) Tangier disease is caused by mutations in the gene encoding ATP-binding cassette transporter 1. *Nat. Genet.* **22**, 352–355
8. Mosser, J., Douar, A. M., Sarde, C. O., Kioschis, P., Feil, R., Moser, H., Poustka, A. M., Mandel, J. L., and Aubourg, P. (1993) Putative X-linked adrenoleukodystrophy gene shares unexpected homology with ABC transporters. *Nature*. **361**, 726–30
9. Zielenski, J., Rozmahel, R., Bozon, D., Kerem, B., Grzelczak, Z., Riordan, J. R., Rommens, J., and Tsui, L.-C. (1991) Genomic DNA sequence of the cystic fibrosis transmembrane conductance regulator (CFTR) gene. *Genomics*. **10**, 214–228
10. Cole, S. P., Bhardwaj, G., Gerlach, J. H., Mackie, J. E., Grant, C. E., Almquist, K. C., Stewart, A. J., Kurz, E. U., Duncan, A. M., and Deeley, R. G. (1992) Overexpression of a transporter gene in a multidrug-resistant human lung cancer cell line. *Science*. **258**, 1650–4
11. Doyle, L. A., Yang, W., Abruzzo, L. V, Krogmann, T., Gao, Y., Rishi, A. K., and Ross, D. D. (1998) A multidrug resistance transporter from human MCF-7 breast cancer cells. *Proc. Natl. Acad. Sci. U. S. A.* **95**, 15665–70
12. Lewis VG1, Ween MP, M. C. (2012) The role of ATP-binding cassette transporters in bacterial pathogenicity. *Protoplasma.* **249(4):**, 919–42
13. Schmidt, K. L., Peterson, N. D., Kustusch, R. J., Wissel, M. C., Graham, B., Phillips, G. J., and Weiss, D. S. (2004) A Predicted ABC Transporter, FtsEX, Is Needed for Cell Division in Escherichia coli. *J. Bacteriol.* **186**, 785–793
14. Paytubi, S., Wang, X., Lam, Y. W., Izquierdo, L., Hunter, M. J., Jan, E., Hundal, H. S., and Proud, C. G. (2009) ABC50 Promotes Translation Initiation in Mammalian Cells. *J. Biol. Chem.* **284**, 24061–24073
15. Cadieux, N., Bradbeer, C., Reeger-Schneider, E., Köster, W., Mohanty, A. K., Wiener, M. C., and Kadner, R. J. (2002) Identification of the periplasmic cobalamin-binding protein BtuF of Escherichia coli. *J. Bacteriol.* **184**, 706–17
16. Yang, J. G., and Rees, D. C. (2015) The allosteric regulatory mechanism of the Escherichia coli MetNI methionine ATP binding cassette (ABC) transporter. *J. Biol. Chem.* **290**, 9135–40
17. Gouridis, G., Schuurman-Wolters, G. K., Ploetz, E., Husada, F., Vietrov, R., de Boer, M., Cordes, T., and Poolman, B. (2015) Conformational dynamics in substrate-binding domains influences transport in the ABC importer GlnPQ. *Nat. Struct. Mol. Biol.* **22**, 57–64
18. Rees, D. C., Johnson, E., and Lewinson, O. (2009) ABC transporters: the power to change. *Nat. Rev. Mol. Cell Biol.* **10**, 218–227
19. Locher, K. P. (2009) Review. Structure and mechanism of ATP-binding cassette transporters. *Philos. Trans. R. Soc. Lond. B. Biol. Sci.* **364**, 239–45
20. Fulyani, F., Schuurman-Wolters, G. K., Zagar, A. V., Guskov, A., Slotboom, D.-J., and Poolman, B. (2013) Functional diversity of tandem substrate-binding domains in ABC transporters from

pathogenic bacteria. *Structure*. **21**, 1879–88
21. Rice, A. J., Park, A., and Pinkett, H. W. (2014) Diversity in ABC transporters: type I, II and III importers. *Crit. Rev. Biochem. Mol. Biol.* **49**, 426–37
22. Smith, P. C., Karpowich, N., Millen, L., Moody, J. E., Rosen, J., Thomas, P. J., and Hunt, J. F. (2002) ATP binding to the motor domain from an ABC transporter drives formation of a nucleotide sandwich dimer. *Mol. Cell*. **10**, 139–49
23. Vigonsky, E., Ovcharenko, E., and Lewinson, O. (2013) Two molybdate/tungstate ABC transporters that interact very differently with their substrate binding proteins. *Proc. Natl. Acad. Sci. U. S. A.* **110**, 5440–5
24. Oldham, M. L., and Chen, J. (2011) Snapshots of the maltose transporter during ATP hydrolysis. *Proc Natl Acad Sci U S A*. **108**, 15152–15156
25. Ames, G. F., Liu, C. E., Joshi, A. K., and Nikaido, K. (1996) Liganded and unliganded receptors interact with equal affinity with the membrane complex of periplasmic permeases, a subfamily of traffic ATPases. *J. Biol. Chem.* **271**, 14264–70
26. Perez, C., Gerber, S., Boilevin, J., Bucher, M., Darbre, T., Aebi, M., Reymond, J.-L., and Locher, K. P. (2015) Structure and mechanism of an active lipid-linked oligosaccharide flippase. *Nature*. **524**, 433–438
27. Herget, M., Kreissig, N., Kolbe, C., Schölz, C., Tampé, R., and Abele, R. (2009) Purification and reconstitution of the antigen transport complex TAP: a prerequisite for determination of peptide stoichiometry and ATP hydrolysis. *J. Biol. Chem.* **284**, 33740–9
28. Kuhnke, G., Neumann, K., Mühlenhoff, U., and Lill, R. (2006) Stimulation of the ATPase activity of the yeast mitochondrial ABC transporter Atm1p by thiol compounds. *Mol. Membr. Biol.* **23**, 173–184
29. Berntsson, R. P.-A., Smits, S. H. J. J., Schmitt, L., Slotboom, D.-J., and Poolman, B. (2010) A structural classification of substrate-binding proteins. *FEBS Lett.* **584**, 2606–17
30. Karpowich, N. K., Huang, H. H., Smith, P. C., and Hunt, J. F. (2003) Crystal structures of the BtuF periplasmic-binding protein for vitamin B12 suggest a functionally important reduction in protein mobility upon ligand binding. *J Biol Chem*. **278**, 8429–8434
31. Teichmann, L., Chen, C., Hoffmann, T., Smits, S. H. J., Schmitt, L., and Bremer, E. (2017) From substrate specificity to promiscuity: hybrid ABC transporters for osmoprotectants. *Mol. Microbiol.* **104**, 761–780
32. Thomas, G. H. (2010) Homes for the orphans: utilization of multiple substrate-binding proteins by ABC transporters. *Mol. Microbiol.* **75**, 6–9
33. Rohrbach, M. R., Braun, V., and Köster, W. (1995) Ferrichrome transport in Escherichia coli K-12: altered substrate specificity of mutated periplasmic FhuD and interaction of FhuD with the integral membrane protein FhuB. *J. Bacteriol.* **177**, 7186–93
34. Woo, J.-S., Zeltina, A., Goetz, B. A., and Locher, K. P. (2012) X-ray structure of the Yersinia pestis heme transporter HmuUV. *Nat. Struct. Mol. Biol.* **19**, 1310–5
35. Borths, E. L., Poolman, B., Hvorup, R. N., Locher, K. P., and Rees, D. C. (2005) In vitro functional characterization of BtuCD-F, the Escherichia coli ABC transporter for vitamin B12 uptake. *Biochemistry*. **44**, 16301–9
36. Kadaba, N. S., Kaiser, J. T., Johnson, E., Lee, A., and Rees, D. C. (2008) The high-affinity E. coli methionine ABC transporter: structure and allosteric regulation. *Science*. **321**, 250–3
37. Gat, O., Mendelson, I., Chitlaru, T., Ariel, N., Altboum, Z., Levy, H., Weiss, S., Grosfeld, H., Cohen, S., and Shafferman, A. (2005) The solute-binding component of a putative Mn(II) ABC transporter (MntA) is a novel Bacillus anthracis virulence determinant. *Mol. Microbiol.* **58**, 533–51
38. Remy, L., Carrière, M., Derré-Bobillot, A., Martini, C., Sanguinetti, M., and Borezée-Durant, E. (2013) The Staphylococcus aureus Opp1 ABC transporter imports nickel and cobalt in zinc-depleted conditions and contributes to virulence. *Mol. Microbiol.* **87**, 730–743
39. McDevitt, C. A., Ogunniyi, A. D., Valkov, E., Lawrence, M. C., Kobe, B., McEwan, A. G., and Paton, J. C. (2011) A Molecular Mechanism for Bacterial Susceptibility to Zinc. *PLoS Pathog*. **7**,

e1002357
40. Rulíšek, L., and Vondrášek, J. (1998) Coordination geometries of selected transition metal ions (Co2+, Ni2+, Cu2+, Zn2+, Cd2+, and Hg2+) in metalloproteins. *J. Inorg. Biochem.* **71**, 115–127
41. Stiefel, E. I. (1996) Transition Metal Sulfur Chemistry: Biological and Industrial Significance and Key Trends, pp. 2–38, 10.1021/bk-1996-0653.ch001
42. Sekowska, A., Kung, H. F., and Danchin, A. (2000) Sulfur metabolism in Escherichia coli and related bacteria: facts and fiction. *J. Mol. Microbiol. Biotechnol.* **2**, 145–77
43. Le Faou, A., Rajagopal, B. S., Daniels, L., and Fauque, G. (1990) Thiosulfate, polythionates and elemental sulfur assimilation and reduction in the bacterial world. *FEMS Microbiol. Rev.* **6**, 351–81
44. Cuhel, R. L., Taylor, C. D., and Jannasch, H. W. (1981) Assimilatory sulfur metabolism in marine microorganisms: characteristics and regulation of sulfate transport in Pseudomonas halodurans and Alteromonas luteo-violaceus. *J. Bacteriol.* **147**, 340–9
45. Uria-Nickelsen, M. R., Leadbetter, E. R., and Godchaux, W. (1994) Sulfonate-sulfur utilization involves a portion of the assimilatory sulfate reduction pathway in Escherichia coli. *FEMS Microbiol. Lett.* **123**, 43–8
46. Lovley, D. R., and Phillips, E. J. (1994) Novel processes for anaerobic sulfate production from elemental sulfur by sulfate-reducing bacteria. *Appl. Environ. Microbiol.* **60**, 2394–9
47. Lochowska, A., Iwanicka-Nowicka, R., Zaim, J., Witkowska-Zimny, M., Bolewska, K., and Hryniewicz, M. M. (2004) Identification of activating region (AR) of Escherichia coli LysR-type transcription factor CysB and CysB contact site on RNA polymerase alpha subunit at the cysP promoter. *Mol. Microbiol.* **53**, 791–806
48. Eichhorn, E., van der Ploeg, J. R., and Leisinger, T. (2000) Deletion Analysis of the Escherichia coli Taurine and Alkanesulfonate Transport Systems. *J. Bacteriol.* **182**, 2687–2695
49. Ohtsu, I., Kawano, Y., Suzuki, M., Morigasaki, S., Saiki, K., Yamazaki, S., Nonaka, G., and Takagi, H. (2015) Uptake of L-cystine via an ABC transporter contributes defense of oxidative stress in the L-cystine export-dependent manner in Escherichia coli. *PLoS One*. **10**, e0120619
50. Chonoles Imlay, K. R., Korshunov, S., and Imlay, J. A. (2015) Physiological Roles and Adverse Effects of the Two Cystine Importers of Escherichia coli. *J. Bacteriol.* **197**, 3629–3644
51. Wolters, J. C., Berntsson, R. P.-A., Gul, N., Karasawa, A., Thunnissen, A.-M. W. H., Slotboom, D.-J., and Poolman, B. (2010) Ligand Binding and Crystal Structures of the Substrate-Binding Domain of the ABC Transporter OpuA. *PLoS One*. **5**, e10361
52. Gilson, E., Alloing, G., Schmidt, T., Claverys, J. P., Dudler, R., and Hofnung, M. (1988) Evidence for high affinity binding-protein dependent transport systems in gram-positive bacteria and in Mycoplasma. *EMBO J.* **7**, 3971–4
53. Masino, L., Martin, S. R., and Bayley, P. M. (2000) Ligand binding and thermodynamic stability of a multidomain protein, calmodulin. *Protein Sci.* **9**, 1519–1529
54. Lo, M.-C., Aulabaugh, A., Jin, G., Cowling, R., Bard, J., Malamas, M., and Ellestad, G. (2004) Evaluation of fluorescence-based thermal shift assays for hit identification in drug discovery. *Anal. Biochem.* **332**, 153–9
55. Damian, L. (2013) Isothermal Titration Calorimetry for Studying Protein–Ligand Interactions. in *Methods in molecular biology (Clifton, N.J.)*, pp. 103–118, **1008**, 103–118
56. Holdgate, G. A. (2001) Making cool drugs hot: isothermal titration calorimetry as a tool to study binding energetics. *Biotechniques*. **31**, 164–6, 168, 170 passim
57. Haber, A., Friedman, S., Lobel, L., Burg-Golani, T., Sigal, N., Rose, J., Livnat-Levanon, N., Lewinson, O., and Herskovits, A. A. (2017) L-glutamine Induces Expression of Listeria monocytogenes Virulence Genes. *PLOS Pathog.* **13**, e1006161
58. Wolf, A., Lee, K. C., Kirsch, J. F., and Ames, G. F.-L. (1996) Ligand-dependent Conformational Plasticity of the Periplasmic Histidine-binding Protein HisJ. *J. Biol. Chem.* **271**, 21243–21250
59. Nguyen, P. T., Lai, J. Y., Lee, A. T., Kaiser, J. T., and Rees, D. C. (2018) Noncanonical role for the binding protein in substrate uptake by the MetNI methionine ATP Binding Cassette (ABC) transporter. *Proc. Natl. Acad. Sci.* **115**, E10596–E10604

60. Vigonsky, E., Fish, I., Livnat-Levanon, N., Ovcharenko, E., Ben-Tal, N., and Lewinson, O. (2015) Metal binding spectrum and model structure of the Bacillus anthracis virulence determinant MntA. *Metallomics*. **7**, 1407–19
61. de Boer, M., Gouridis, G., Vietrov, R., Begg, S. L., Schuurman-Wolters, G. K., Husada, F., Eleftheriadis, N., Poolman, B., McDevitt, C. A., and Cordes, T. (2019) Conformational and dynamic plasticity in substrate-binding proteins underlies selective transport in ABC importers. *Elife*. 10.7554/eLife.44652
62. Bordignon, E., Grote, M., and Schneider, E. (2010) The maltose ATP-binding cassette transporter in the 21st century--towards a structural dynamic perspective on its mode of action. *Mol. Microbiol.* **77**, 1354–66
63. Kerppola, R. E., Shyamala, V. K., Klebba, P., and Ames, G. F. (1991) The membrane-bound proteins of periplasmic permeases form a complex. Identification of the histidine permease HisQMP complex. *J. Biol. Chem.* **266**, 9857–65
64. van der Heide, T., and Poolman, B. (2000) Osmoregulated ABC-transport system of Lactococcus lactis senses water stress via changes in the physical state of the membrane. *Proc. Natl. Acad. Sci. U. S. A.* **97**, 7102–6
65. Lanfermeijer, F. C., Picon, A., Konings, W. N., and Poolman, B. (1999) Kinetics and consequences of binding of nona- and dodecapeptides to the oligopeptide binding protein (OppA) of Lactococcus lactis. *Biochemistry*. **38**, 14440–50
66. Rice, A. J., Alvarez, F. J. D., Schultz, K. M., Klug, C. S., Davidson, A. L., and Pinkett, H. W. (2013) EPR spectroscopy of MolB2C2-a reveals mechanism of transport for a bacterial type II molybdate importer. *J. Biol. Chem.* **288**, 21228–35
67. Sebulsky, M. T., Shilton, B. H., Speziali, C. D., and Heinrichs, D. E. (2003) The role of FhuD2 in iron(III)-hydroxamate transport in Staphylococcus aureus. Demonstration that FhuD2 binds iron(III)-hydroxamates but with minimal conformational change and implication of mutations on transport. *J. Biol. Chem.* **278**, 49890–900
68. Mattle, D., Zeltina, A., Woo, J.-S., Goetz, B. A., and Locher, K. P. (2010) Two stacked heme molecules in the binding pocket of the periplasmic heme-binding protein HmuT from Yersinia pestis. *J. Mol. Biol.* **404**, 220–31
69. Liu, C. E., Liu, P. Q., and Ames, G. F. (1997) Characterization of the adenosine triphosphatase activity of the periplasmic histidine permease, a traffic ATPase (ABC transporter). *J. Biol. Chem.* **272**, 21883–91
70. Davidson, A. L., Shuman, H. A., and Nikaido, H. (1992) Mechanism of maltose transport in Escherichia coli: transmembrane signaling by periplasmic binding proteins. *Proc. Natl. Acad. Sci. U. S. A.* **89**, 2360–4
71. Patzlaff, J. S., van der Heide, T., and Poolman, B. (2003) The ATP/substrate stoichiometry of the ATP-binding cassette (ABC) transporter OpuA. *J. Biol. Chem.* **278**, 29546–51
72. Tal, N., Ovcharenko, E., and Lewinson, O. (2013) A single intact ATPase site of the ABC transporter BtuCD drives 5% transport activity yet supports full in vivo vitamin B12 utilization. *Proc. Natl. Acad. Sci. U. S. A.* **110**, 5434–9
73. Locher, K. P., Lee, A. T., Rees, D. C., and Lee AT, R. D. L. K. (2002) The E. coli BtuCD structure: a framework for ABC transporter architecture and mechanism. *Science (80-.).* **10**, 1091–8
74. Davidson, A. L., Laghaeian, S. S., and Mannering, D. E. (1996) The maltose transport system of Escherichia coli displays positive cooperativity in ATP hydrolysis. *J. Biol. Chem.* **271**, 4858–63
75. Bennett, B. D., Kimball, E. H., Gao, M., Osterhout, R., Van Dien, S. J., and Rabinowitz, J. D. (2009) Absolute metabolite concentrations and implied enzyme active site occupancy in Escherichia coli. *Nat. Chem. Biol.* **5**, 593–9
76. Spurlino, J. C., Lu, G. Y., and Quiocho, F. A. (1991) The 2.3-A resolution structure of the maltose- or maltodextrin-binding protein, a primary receptor of bacterial active transport and chemotaxis. *J. Biol. Chem.* **266**, 5202–19
77. Sun, Y. J., Rose, J., Wang, B. C., and Hsiao, C. D. (1998) The structure of glutamine-binding

protein complexed with glutamine at 1.94 A resolution: comparisons with other amino acid binding proteins. *J. Mol. Biol.* **278**, 219–29
78. Hsiao, C. D., Sun, Y. J., Rose, J., and Wang, B. C. (1996) The crystal structure of glutamine-binding protein from Escherichia coli. *J. Mol. Biol.* **262**, 225–42
79. Mao, B., Pear, M. R., McCammon, J. A., and Quiocho, F. A. (1982) Hinge-bending in L-arabinose-binding protein. The "Venus's-flytrap" model. *J. Biol. Chem.* **257**, 1131–3
80. Merino, G., Boos, W., Shuman, H. A., and Bohl, E. (1995) The Inhibition of Maltose Transport by the Unliganded Form of the Maltose-binding Protein ofEscherichia coli: Experimental Findings and Mathematical Treatment. *J. Theor. Biol.* **177**, 171–179
81. Remmert, M., Biegert, A., Hauser, A., and Söding, J. (2011) HHblits: lightning-fast iterative protein sequence searching by HMM-HMM alignment. *Nat. Methods.* **9**, 173–5
82. Mirdita, M., Von Den Driesch, L., Galiez, C., Martin, M. J., Soding, J., and Steinegger, M. (2017) Uniclust databases of clustered and deeply annotated protein sequences and alignments. *Nucleic Acids Res.* **45**, D170–D176
83. Katoh, K., and Standley, D. M. (2016) A simple method to control over-alignment in the MAFFT multiple sequence alignment program. *Bioinformatics*. **32**, 1933–1942
84. Šali, A., and Blundell, T. L. (1993) Comparative protein modelling by satisfaction of spatial restraints. *J. Mol. Biol.* **234**, 779–815
85. Bulut, H., Moniot, S., Licht, A., Scheffel, F., Gathmann, S., Saenger, W., and Schneider, E. (2012) Crystal Structures of Two Solute Receptors for l-Cystine and l-Cysteine, Respectively, of the Human Pathogen Neisseria gonorrhoeae. *J. Mol. Biol.* **415**, 560–572
86. Ashkenazy, H., Abadi, S., Martz, E., Chay, O., Mayrose, I., Pupko, T., and Ben-Tal, N. (2016) ConSurf 2016: an improved methodology to estimate and visualize evolutionary conservation in macromolecules. *Nucleic Acids Res.* **44**, W344-50
87. de Boer, M., Gouridis, G., Muthahari, Y. A., and Cordes, T. (2019) Single-Molecule Observation of Ligand Binding and Conformational Changes in FeuA. *Biophys. J.* **117**, 1642–1654
88. Oldham, M. L., and Chen, J. (2011) Crystal structure of the maltose transporter in a pretranslocation intermediate state. *Science*. **332**, 1202–5
89. Mächtel, R., Narducci, A., Griffith, D. A., Cordes, T., and Orelle, C. (2019) An integrated transport mechanism of the maltose ABC importer. *Res. Microbiol.* 10.1016/j.resmic.2019.09.004
90. Paul, S., Banerjee, S., and Vogel, H. J. (2017) Ligand binding specificity of the Escherichia coli periplasmic histidine binding protein, HisJ. *Protein Sci.* **26**, 268–279
91. Nguyen, P. T., Lai, J. Y., Kaiser, J. T., and Rees, D. C. (2019) Structures of the Neisseria meningitides methionine-binding protein MetQ in substrate-free form and bound to l - and d - methionine isomers. *Protein Sci.* **28**, 1750–1757
92. Quadroni, M., Staudenmann, W., Kertesz, M., and James, P. (1996) Analysis of global responses by protein and peptide fingerprinting of proteins isolated by two-dimensional gel electrophoresis. Application to the sulfate-starvation response of Escherichia coli. *Eur. J. Biochem.* **239**, 773–781
93. Soutourina, J., Blanquet, S., and Plateau, P. (2001) Role of D-Cysteine Desulfhydrase in the Adaptation of Escherichia coli to D-Cysteine. *J. Biol. Chem.* **276**, 40864–40872
94. Madhavi Sastry, G., Adzhigirey, M., Day, T., Annabhimoju, R., and Sherman, W. (2013) Protein and ligand preparation: Parameters, protocols, and influence on virtual screening enrichments. *J. Comput. Aided. Mol. Des.* **27**, 221–234
95. Greenwood, J. R., Calkins, D., Sullivan, A. P., and Shelley, J. C. (2010) Towards the comprehensive, rapid, and accurate prediction of the favorable tautomeric states of drug-like molecules in aqueous solution. *J. Comput. Aided. Mol. Des.* **24**, 591–604
96. Friesner, R. A., Murphy, R. B., Repasky, M. P., Frye, L. L., Greenwood, J. R., Halgren, T. A., Sanschagrin, P. C., and Mainz, D. T. (2006) Extra precision glide: Docking and scoring incorporating a model of hydrophobic enclosure for protein-ligand complexes. *J. Med. Chem.* **49**, 6177–6196
97. Wang, L., Li, L., and Alexov, E. (2015) pKa predictions for proteins, RNAs, and DNAs with the Gaussian dielectric function using DelPhi pKa. *Proteins Struct. Funct. Bioinforma.* **83**, 2186–2197

Figure 1

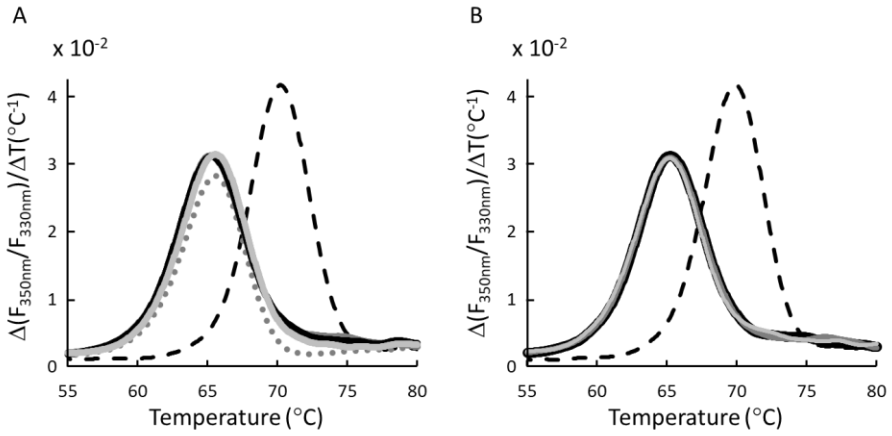

Figure 1. Binding of sulfur-containing compounds by FliY. Shown are nanoDSF measurements conducted with 30 µM FliY in the presence of 200 µM of the following: (A) no addition (apo FliY, solid black trace), L- cysteine (dashed black trace), L- serine (light grey, solid), L- methionine (light grey, dotted), or glutathione (dark grey, solid). (B) same as in A, only shown are the measurements for apo FliY (no addition, solid black trace), L- cystine (dashed black trace), D- cystine (light grey, solid), D- cysteine (dark grey, solid). Shown are representative experiments conducted at least three times.

Figure 2

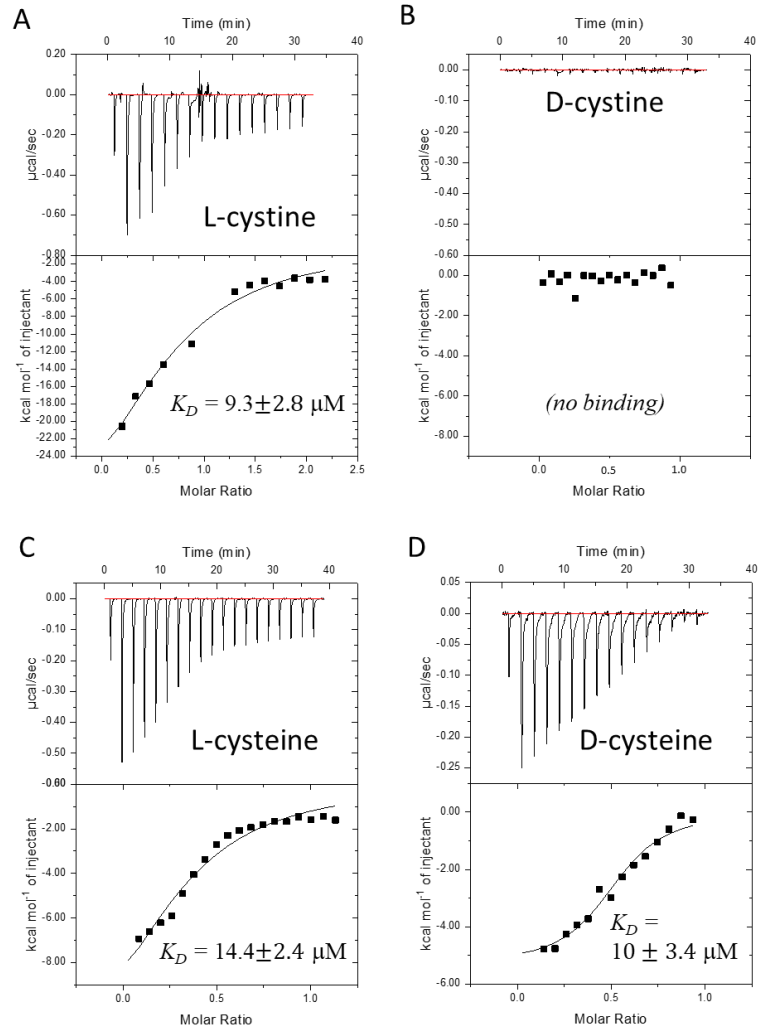

Figure 2. Affinity of binding of the D/L enantiomers of cystine and cysteine. Isothermal titration calorimetry was used to determine the binding of L-cystine (A), D-cystine (B), L-cysteine (C), or D-cysteine (D). Shown are the consecutive injections of 2 µL aliquots from a 200-400 µM solutions of the indicated amino acid, into 200 µL of 70 µM FliY. The top panels show the calorimetric titration and the bottom panels display the integrated injection heat derived from the titrations, for which the best-fit curve (solid black trace) was used to calculate the K_D. The experiments were conducted three times, and the K_D value is mean ±SD of 3 independent experiments.

Figure 3

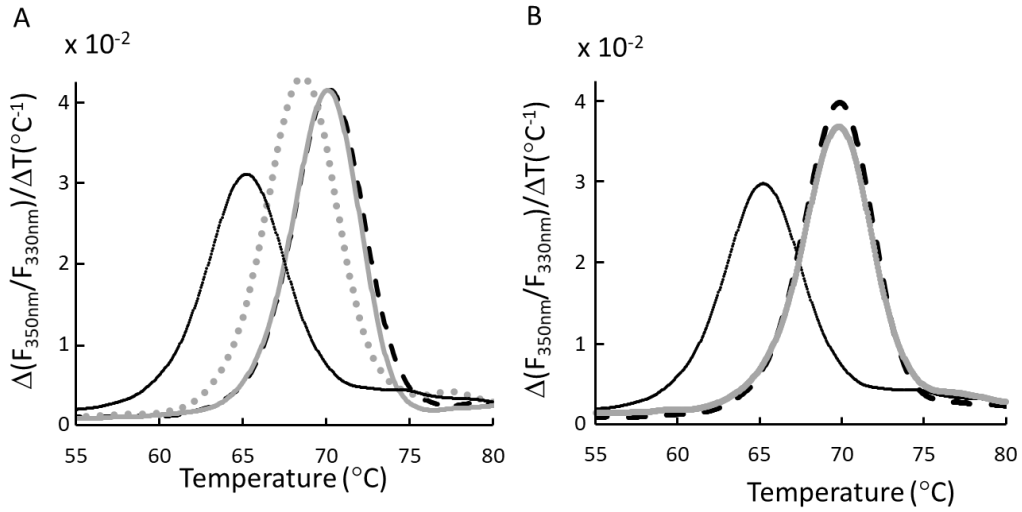

Figure 3. Competition between the D and L enantiomers of cystine and cysteine in binding to FliY. Shown are nanoDSF competition measurements conducted with 10 µM FliY under the following conditions (A) no addition (apo FliY, solid black trace), 50 µM L- cysteine (dashed black trace), 50 µM L- cysteine and 200 µM D- cysteine (light grey, dotted), or 50 µM L- cysteine and 200 µM L- methionine (light grey, solid). (B) no addition (apo FliY, solid black trace), 50 µM L- cystine (dashed black trace), or 50 µM L-cystine and 200 µM D- cystine (light grey, solid).

Figure 4

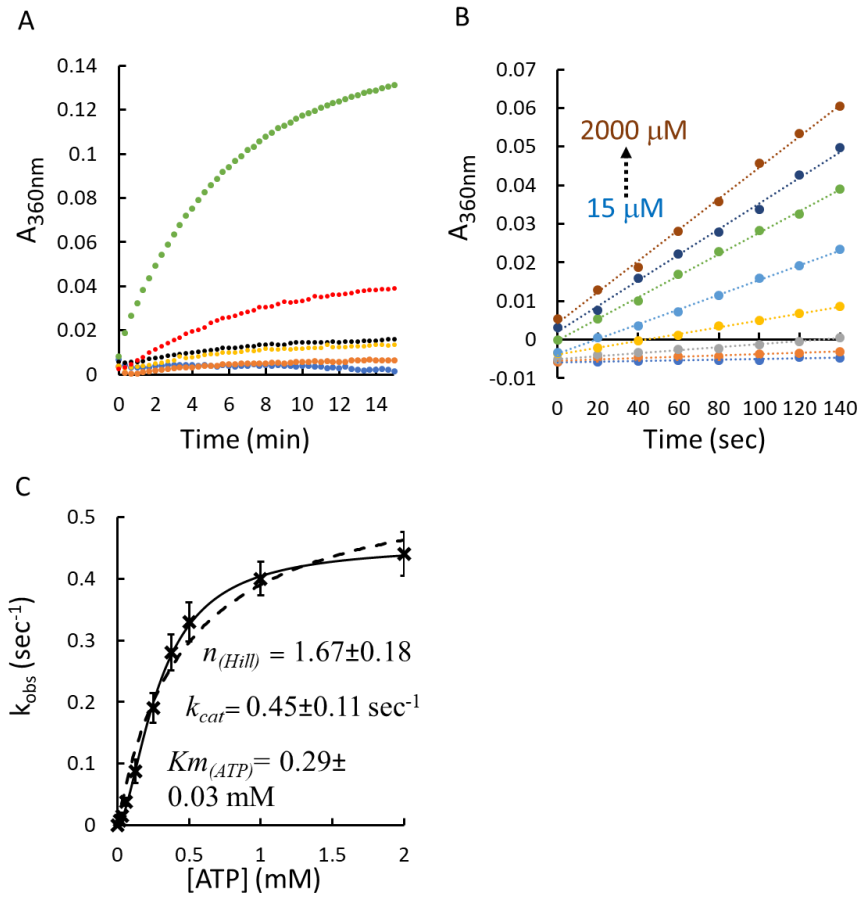

Figure 4. ATP hydrolysis by YecSC. (A) 0.5 µM of purified YecSC was supplemented with 10 µM of *E. coli* polar lipids and incubated for 2 min with 1mM ATP. To initiate hydrolysis 2mM $MgSO_4$ were injected at time zero. The rate of release of inorganic phosphate was determined by continuous monitoring of the 340 nm absorbance of the solution using the EnzCheck kit. ATP hydrolysis was measured in the presence of 0.5 µM YecSC (black curve), buffer only (blue), 1 µM FliY (orange), 0.5 µM YecSC and 30 µM L-cystine (yellow), 0.5 µM YecSC and 1 µM FliY (red), or 0.5 µM YecSC, 1 µM FliY and 30 µM L- cystine (green). Shown are representative experiments conducted at least three times. (B) Initial rates of hydrolysis of 15-1000 µM ATP were measured in the presence of 1 µM YecSC, 5 µM FliY and 100 µM L- cystine. Circles represent the experimental data and the dotted lines are the linear fits. (C) The initial rates of ATP hydrolysis were plotted as a function of the ATP concentration (crosses). The data was then fit using the Michaelis–Menten equation (dashed line) or its expanded version that includes also a term for the Hill coefficient (solid line).

Figure 5

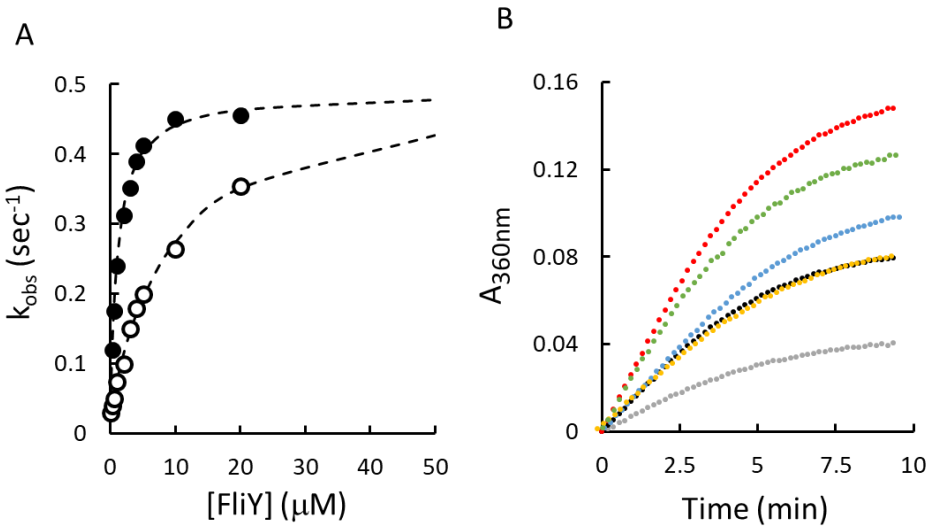

Figure 5. (A) Modulation of ATP hydrolysis by apo- and holo-FliY. ATP hydrolysis by 1 μM YecSC was measured in the presence of a range of FliY concentrations (0.25-20 μM, as indicated) in the absence (empty circles) or presence (full circles) of 100 μM L- cystine. The dashed line represents the fit of the data using the Michaelis–Menten. (B) Stimulation of the ATPase activity by the D and L enantiomers. ATP hydrolysis was measured for 1 μM YecSC (grey), 1 μM YecSC and 2 μM FliY (black), 1 μM YecSC, 2 μM FliY, and 30 μM D- cystine (yellow), 1 μM YecSC, 2 μM FliY, and 30 μM D- cysteine (blue), 1 μM YecSC, 2 μM FliY, and 30 μM L- cysteine (green), or 1 μM YecSC, 2 μM FliY, and 30 μM L- cystine (red).

Figure 6

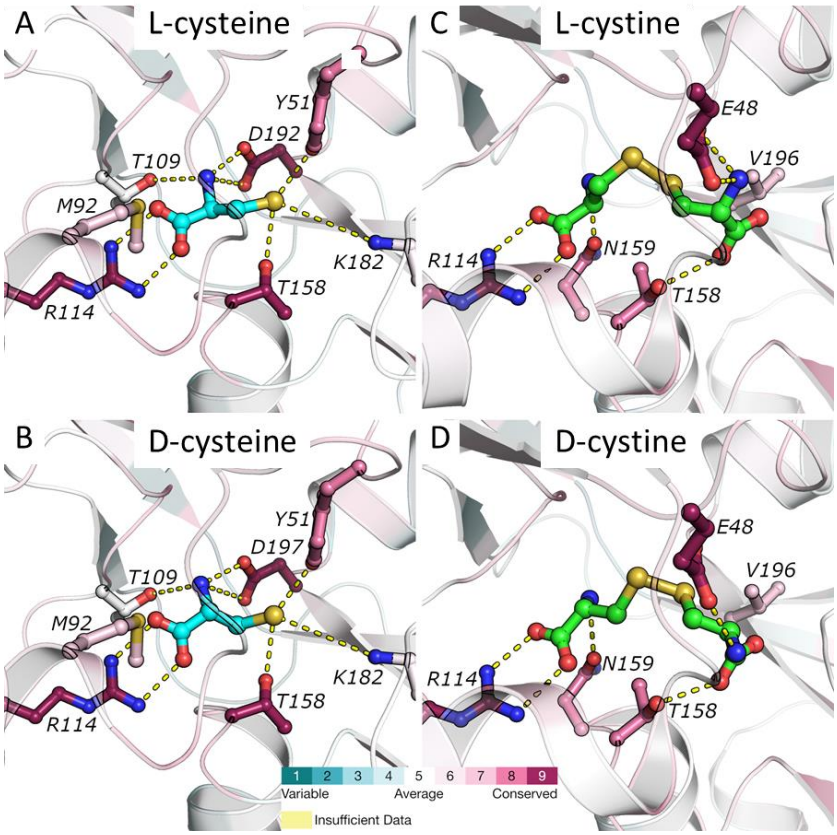

Figure 6. 3-D modeling of FliY and enantiomer coordination. FliY was modelled based on the structures of the L-cysteine SBP (A, B, PDB ID: 2YJP) or the L-cystine SBP (C, D, PDB ID: 2YLN). The protein backbone is shown as a cartoon representation and selected ligand-coordinating residues are shown as ball and sticks, colored according to their ConSurf conservation score. The ligands are shown as ball and sticks and are colored cyan (L-cysteine, A, D-cysteine, B) or green (L-cystine, C, D-cystine, D). Also shown at the bottom is the ConSurf color-coded conservation scale (1-variable, 9-conserved)

Figure 7

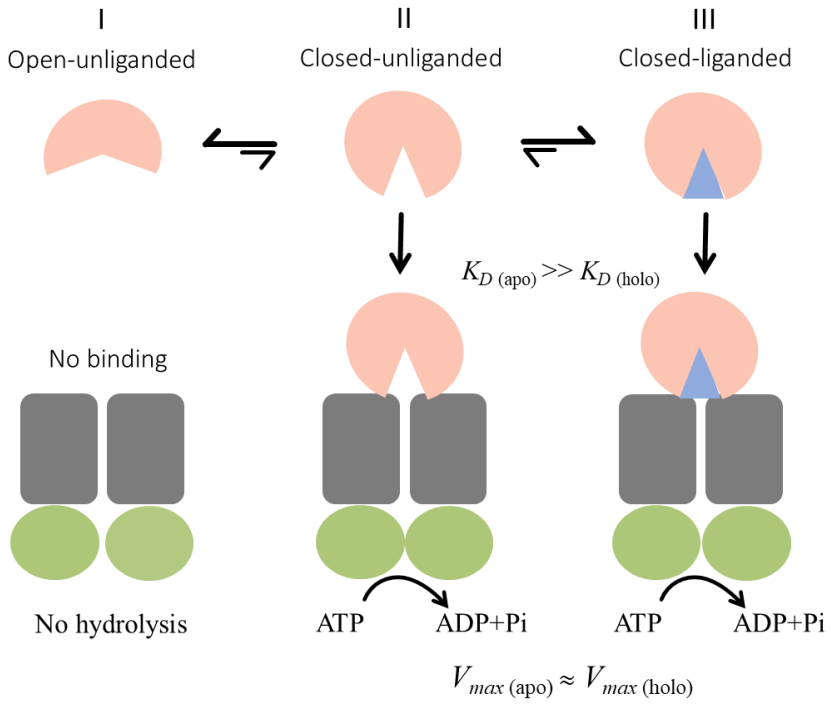

Figure 7. Proposed model for the YecSC-FliY interaction and modulation of ATPase activity. In the absence of ligand, FliY exists in a conformational equilibrium between open- and closed-unliganded forms, where the majority of the molecules are in the open form (state I). The molecules that are in state I do not interact with the transporter and do not stimulate its ATPase activity. The minority of molecules that are in the closed-unliganded form (state II) interact with the transporter and stimulate its ATPase activity. When ligand is present, its binding induces a population shift towards the closed-liganded form (state III). More molecules are not available for interaction with the transporter and higher ATPase stimulation is observed. Nevertheless, even in the absence of substrate, when the concentrations of apo-FliY are sufficiently high, the concentration of the fraction of the molecules that are in the closed-unliganded form will be higher than the K_D for interaction of YecSC with the closed-unliganded FliY and also higher than the concentration of YecSC. Therefore, maximal ATPase rates are achieved ($V_{max\ (apo)} \approx V_{max\ (holo)}$) and further addition of substrate does not lead to increased activity. $K_{D\ (apo)}$ and $K_{D\ (holo)}$ represent the apparent K_D for the FliY-YecSC interaction (in the absence or presence of substrate, respectively) as inferred from the apparent K_M of FliY-mediated stimulation of ATPase activity.

Substrate recognition and ATPase activity of the E. coli cysteine/cystine ABC transporter YecSC-FliY

Siwar Sabrialabe, Janet G Yang, Elon Yariv, Nir Ben-Tal and Oded Lewinson

J. Biol. Chem. published online March 6, 2020
